

CHANGES IN SENSITIVITY OF THE LOW DISPERSION MODES

Ralph Bohlin
November 1999

ABSTRACT

Significant changes in the STIS sensitivity are revealed by 2.3 years of observations of the same standard stars in the 52X2 arcsec slit. The largest changes are in G140L, where the sensitivity depends on both the time and temperature. The minor effect is a -0.25%/C temperature correlation, where the bulk of the observations are confined to the 34.5-38.5C temperature range. No significant change with temperature is detected for the near-UV MAMA or CCD modes.

Following a correction for the correlation with temperature, the sensitivity of G140L decreases linearly with time. These losses vary with wavelength, ranging from a minimum of -0.8%/yr at 1325Å to a maximum of -2.8%/yr at 1575Å. For G230L, the mean sensitivity over all wavelengths increases by an average of 1.8% in the first 1.3 years and then begins to drop. Two straight lines with different slopes fit the observed changes. The changes before 1998.7 also vary with wavelength, ranging from a minimum of +0.8%/yr at 2550 to a maximum at 2250Å of +2.1%/yr. The wavelength-dependent slopes of the currently decreasing sensitivity range from zero at the short wavelength end of the band to -1.9%/yr in the 2300-2400Å interval. Changes in the three low dispersion CCD modes are less severe. For G230LB and G750L, most wavelength bins are consistent within a three σ uncertainty of constant sensitivity over time. Only one wavelength bin for G230LB and two for G750L show sensitivity losses with more than three σ certainty. Those changes are small and lie in the 0.2-0.4%/yr range. However for G430L, the losses in every 200Å wavelength bin beyond 3300Å range from 0.5 to 0.7%/yr with a high statistical significance of 2-9 σ .

After correcting the three low-dispersion modes for sensitivity changes, the 1 σ photometric broadband repeatability ranges from 0.2% for G140L and G750L to 0.4% for spectrophotometry in the other 3 modes.

1. INTRODUCTION

The entire data set of 2.3 years has been uniformly reprocessed with current spectral extraction techniques. The analysis is confined to a single star for each mode, i.e. GRW+70D5824 for the MAMA modes and AGK+81D266 for the CCD modes, rather than including the standard star photometry of GD153, GD71, and G191B2B per Walborn and Bohlin (1998, WB). The first year of the WB sensitivity monitoring observations comprised a small data set that required the supplemental data from a variety of stars. The new results are usually consistent with the previous WB results to 1-2 σ and within 3 σ in all cases for the larger uncertainties of the first year's data. With the additional 1.3 years of monitoring, the refined processing, and a purer data set than WB, the rates of sensitivity change now have uncertainties that are reduced by factors of 2-3 typically, or by as much as a factor of six for G750L.

2. OBSERVATIONS

Since the repeatability was studied by WB and since the absolute calibration was defined by Bohlin, Collins, and Gonnella (1998), more low-dispersion monitoring observations have been made and are listed in Table 1. Table 1 contains all of the new observations of GRW+70D5824 for the MAMA modes and AGK+81D266 for the CCD modes that are not tabulated by WB. All CCD observations are at gain=1 with CRSPLIT=2, and all G750L observations have contemporaneous short slit tungsten flats for fringe removal. The custom IDL programs TCORREL and MAKE_TCHANG have been developed for the analysis of these observations.

Table 1. New L-Mode Monitoring Observations

ROOT	MODE	APER	TARGET	DATE	TIME	PROPID	EXPTIME
O45944010	G140L	52X2	GRW+70D584	23/09/98	08:02:51	7673	204.0
O45944020	G230L	52X2	GRW+70D584	23/09/98	08:13:10	7673	204.0
O45945010	G140L	52X2	GRW+70D584	14/10/98	22:40:39	7673	204.0
O45945020	G230L	52X2	GRW+70D584	14/10/98	22:50:58	7673	204.0
O45946010	G140L	52X2	GRW+70D584	04/11/98	06:35:51	7673	204.0
O45946020	G230L	52X2	GRW+70D584	04/11/98	06:46:10	7673	204.0
O45947010	G140L	52X2	GRW+70D584	14/12/98	14:51:39	7673	204.0
O45947020	G230L	52X2	GRW+70D584	14/12/98	15:01:58	7673	204.0
O45948010	G140L	52X2	GRW+70D584	99-01-03	08:36:14	7673	204.0
O45948020	G230L	52X2	GRW+70D584	99-01-03	08:46:33	7673	204.0
O45949010	G140L	52X2	GRW+70D584	99-02-11	12:54:13	7673	204.0

STIS Instrument Science Report 99-07

ROOT	MODE	APER	TARGET	DATE	TIME	PROPID	EXPTIME
O45949020	G230L	52X2	GRW+70D584	99-02-11	13:04:32	7673	204.0
O45950010	G140L	52X2	GRW+70D584	99-03-08	16:55:02	7673	204.0
O45950020	G230L	52X2	GRW+70D584	99-03-08	17:05:21	7673	204.0
O45951010	G140L	52X2	GRW+70D584	99-04-11	05:52:14	7673	204.0
O45951020	G230L	52X2	GRW+70D584	99-04-11	06:02:33	7673	204.0
O45952010	G140L	52X2	GRW+70D584	99-05-12	18:15:58	7673	204.0
O45952020	G230L	52X2	GRW+70D582	99-05-12	18:26:17	7673	204.0
O45953010	G140L	52X2	GRW+70D584	99-06-03	02:08:16	7673	204.0
O45953020	G230L	52X2	GRW+70D584	99-06-03	02:18:35	7673	204.0
O5JJ01010	G140L	52X2	GRW+70D584	99-07-03	08:44:21	8424	201.0
O5JJ01020	G230L	52X2	GRW+70D584	99-07-03	08:54:37	8424	204.0
O5JJ02010	G140L	52X2	GRW+70D584	99-08-03	00:32:16	8424	204.0
O5JJ02020	G230L	52X2	GRW+70D584	99-08-03	00:42:35	8424	204.0
O5JJ03010	G140L	52X2	GRW+70D582	99-09-18	00:30:05	8424	201.0
O5JJ03020	G230L	52X2	GRW+70D584	99-09-18	00:40:21	8424	204.0
O5JJ99010	G140L	52X2	GRW+70D584	99-10-01	18:14:28	8424	204.0
O5JJ99020	G230L	52X2	GRW+70D584	99-10-01	18:24:47	8424	204.0
O5JJ99030	G140L	52X2	GRW+70D584	99-10-01	18:35:41	8424	204.0
O45A14010	G230LB	52X2	AGK+81D266	12/10/98	12:29:56	7672	172.8
O45A14020	G430L	52X2	AGK+81D266	12/10/98	12:39:05	7672	172.8
O45A14030	G750L	52X2	AGK+81D266	12/10/98	12:48:14	7672	432.0
O45A15010	G230LB	52X2	AGK+81D266	06/12/98	22:46:56	7672	172.8
O45A15020	G430L	52X2	AGK+81D266	06/12/98	22:56:11	7672	172.8
O45A15030	G750L	52X2	AGK+81D266	06/12/98	23:05:26	7672	432.0
O45A16010	G230LB	52X2	AGK+81D266	99-02-07	00:36:26	7672	172.8
O45A16020	G430L	52X2	AGK+81D266	99-02-07	00:45:41	7672	172.8
O45A16030	G750L	52X2	AGK+81D266	99-02-07	00:54:56	7672	432.0
O45A17010	G230LB	52X2	AGK+81D266	99-04-03	15:30:29	7672	172.8
O45A17020	G430L	52X2	AGK+81D266	99-04-03	15:39:44	7672	172.8
O45A17030	G750L	52X2	AGK+81D266	99-04-03	15:48:59	7672	432.0
O45A18010	G230LB	52X2	AGK+81D266	99-06-03	13:29:36	7672	172.8
O45A18020	G430L	52X2	AGK+81D266	99-06-03	13:38:51	7672	172.8

ROOT	MODE	APER	TARGET	DATE	TIME	PROPID	EXPTIME
O45A18030	G750L	52X2	AGK+81D266	99-06-03	13:48:06	7672	432.0
O5IG01010	G230LB	52X2	AGK+81D266	99-08-01	01:16:42	8418	172.8
O5IG01020	G430L	52X2	AGK+81D266	99-08-01	01:25:57	8418	172.8
O5IG01030	G750L	52X2	AGK+81D266	99-08-01	01:35:12	8418	432.0
O5IG02010	G230LB	52X2	AGK+81D266	99-10-03	02:14:59	8418	172.8
O5IG02020	G430L	52X2	AGK+81D266	99-10-03	02:24:14	8418	172.8
O5IG02030	G750L	52X2	AGK+81D266	99-10-03	02:33:29	8418	432.0

3. TEMPERATURE CORRELATIONS

As the first step, the broadband response over the range of the bulk of the detector response is examined for time and temperature correlations via a multiple regression analysis in the IDL program TCORREL. For example, G140L uses the wavelength range 1300-1650Å to avoid Ly-alpha. For the MAMA's, the charge amplifier temperature, OM1CAT and OM2CAT are the measures of temperature. Checks with other temperatures in the MAMA1 electronic chain are consistent with the OM1CAT result of $-0.25\%/C \pm 0.05$ for G140L. For G230L and OM2CAT, the result is $0.08\%/C \pm 0.06$ without time correction and 0.03 ± 0.02 after making the time correction (see section 4) before doing the regression fit. Special tests for wavelength dependence are made in selected narrow wavelength bands. Those results are all consistent with the broadband temperature correlations.

For the CCD modes, the CCDTEMP must be extracted from the engineering data stream. Unfortunately, the temperature is digitized and recorded to $\sim 0.8C$ precision, while the total range of CCD temperature fluxuation is only $\sim 1.5C$, i.e. just 2-3 digitization steps. No correlation with temperature is detected; however, the precision limits are coarser than the 1σ uncertainty of $\pm 0.05\%/C$ for G140L. The formal 3σ upper limits are $0.6\%/C$ for G230LB and G750L and $0.9\%/C$ for G430L. Assuming wavelength independence and combining the three CCD modes gives a 3σ upper limit on sensitivity change with temperature of $0.4\%/C$.

No correction for change with temperature is needed for G230L or for the CCD modes, while the G140L correlation is significant at the five σ level and has been applied before conducting the linear regression studies of changes vs. time in the following section. Since the bulk of the observations lie in the 34-38C range, the G140L temperature change of $-0.25\%/C$ is normalized to unity at 36C. Thus, the corrections are commonly in the $\pm 0.5\%$ range, while the most extreme temperature of 30.4C implies an increase of response of 1.4% and requires a multiplication of the photometry by 0.986 to get to the standard 36C reference temperature. Following installation of the new cooling system on

SM-3B, a decrease in the MAMA operating temperature of 15-20C is expected (R. Kimble private communication) and should produce an increase in the FUV-MAMA sensitivity of 4-5%.

4. TIME CORRELATIONS

Following implementation of the TCORREL results, the software tool MAKE-TCHANG displays the changes in sensitivity as a function of time and writes the files of change coefficients. MAKE-TCHANG plots appear in Figures 1-5 and show the changes in 11-13 wavelength bins for each of the five low dispersion modes. The large diamonds represent the ratio of each observation to the average spectrum of GRW+70D5824 for the MAMAs and of AGK+81D266 for the CCD modes. Only the diamonds are used to derive the time changes; the WD data are displayed only to demonstrate the agreement of the absolute flux standards with the main set of observations obtained for the purpose of monitoring the time changes. The solid straight lines are least square fits to the diamonds, where the slope and 1σ uncertainty in the slope are written on the panel for each wavelength bin. Also written on each panel are the central wavelength of each bin and the 1σ rms scatter in the data before and after correction by the fit.

While the monthly MAMA dither offset is zero for the GRW+70D5824 observations in order to avoid small changes in sensitivity, the standard spectral y-location for G140L was changed from +3 arcsec to -3 arcsec on 99Mar15 (1999.20). The small scatter in the spectral y-position of a couple of pixels perpendicular to the dispersion does not cause a problem; but the shift in the standard position from +3 to -3 arcsec produces a systematic change in response for G140L spectra taken after 99Mar15. In Table 1, O5JJ99030 taken on 99Oct1 is a special observation at the +3 arcsec position. In order to measure the mean ratio of the +3 to -3 sensitivities, a preliminary version of the G140L time corrections is derived and implemented using just the 22 observations at +3 arcsec. Then, the average of the 22 corrected G140L observation at +3 is ratioed to the average of the 7 spectra at -3 arcsec, as corrected with the same time and temperature coefficients. This ratio is fit with a 12 node spline function as illustrated in Figure 6. The -3 position spectra are corrected by the spline fit and included in the fit of Figure 1. A new ratio of +3 to -3 sensitivities is calculated and the process is iterated a couple of times to demonstrate convergence to <0.1% in the time changes. In the next millennium, the assumption that the same time and temperature changes apply everywhere on the FUV-MAMA should be verified with a longer baseline than the 99Apr11-99Oct1 observations at -3 arcsec.

For G230L in Figure 2, the sensitivity first increases and then begins to decrease around 1998.7, as is more clearly illustrated in the analogous Figure 7 of the changes averaged over 1900-2900Å. This broadband photometric repeatability before and after correction by the straight line fits is written on the Figure 7 and collected in Table 2, along with the analogous values for the other modes. Figure 2 shows that all wavelength bins

have initial sensitivity increases with statistical uncertainties at the 3-11 σ level. After 1998.7, the four short wavelength regions covering 1700-2000Å are consistent with a constant sensitivity. A physical explanation for these trends could be that initially, an evaporation of external contaminants or an internal scrubbing or migration of cathode material into the microchannel-plate pores in the NUV-MAMA dominated over the usual losses that are caused by polymerized hydrocarbons that gradually collect on the optical surfaces.

Table 2. Average Photometric Precision over Broad Wavelength Ranges for the 52x2 Arcsec Slit

Mode	Bandpass	1 σ (%)	1 σ (%)
	(Å)	(before)	(after)
G140L	1300-1650	1.58	0.44
G230L	1900-2900	0.55	0.15
G230LB	2000-3000	0.38	0.38*
G430L	3500-5500	0.55	0.38
G750L	5500-8300	0.24	0.17*

* Corrections for sensitivity changes are not large enough or statistically significant enough to implement.

The changes in sensitivity of the CCD modes are smaller than for the MAMA modes. The average changes for the G230LB and G750L are <0.3%/yr, which are comparable to other uncertainties. Only two of the 13 individual G230LB wavelength bins show changes of >0.4%/yr with a 2-3 σ statistical significance. For G750L, four of the 11 individual bins change at >0.4%/yr with a 2-3 σ statistical significance; but these bins are in the 8000-9000Å range where other uncertainties are larger.

Only for the CCD G430L mode is the evidence for sensitivity change compelling enough to warrant correction. The average change is -0.56%/yr +/- 0.16, while 10 of the 13 wavelength bins decline at >0.4%/yr with an uncertainty of better than 2 σ . Seven of these 10 changes are significant at the 3-9 σ level, as shown in Figure 4. The confinement of significant sensitivity loss to the 3500-5600Å range on the CCD is curious and suggests that the cause might be associated with the order blocking filter on the G430L grating.

The changes over time are all normalized to unity at 1997.38, the starting time of calibration observations and close to the time of the initial epoch calibration of Bohlin, Collins & Gonnella (1998), so that the changes in the absolute sensitivity calibration (Bohlin in preparation) can be attributed to other factors than changes with time. The large and statistically significant changes for the three low-dispersion modes are summarized in Figures 8-10 at half year increments from 1997.38 to 2000.38. The physical reality of the

observed changes is emphasized by the continuity of the curves as a function of wavelength in Figures 8-10, since there is no smoothing in the analysis that constrains the continuity.

The reality of the wavelength dependent changes is further evidenced by the monitoring of two medium dispersion G140M modes (Smith, Walborn, & Stys private communication.) G140M-1173 (1150-1190Å) and G140M-1567 (1542-1592Å) have changes over time that are consistent with the similar G140L waveband in Figure 1. For example, the G140M-1567 mode with the smallest uncertainty and longest baseline from 97Sep-99Mar declines at -2.2 ± 0.4 %/yr, while the 1550-1600Å band in Figure 1 shows a -2.8 ± 0.2 %/yr loss.

5. RECOMMENDATIONS

The time and temperature correlations are now known to sufficient precision to justify inclusion in the pipeline data processing for the extracted absolute flux of point sources in three of the five low dispersion modes. The uncorrected net count rates should be retained so that corrections would not need to be backed out following updates of the correction coefficients. The latest file of correction coefficients in terms of the value of the correction at the endpoints of the straight line fits should be available on-line for the few cases where the corrections themselves are required. The medium and echelle modes may have the same sensitivity change as a function of wavelength but corrections are not required, since the high dispersion modes are rarely used to obtain accurate spectrophotometry. The linear extrapolation of the time changes by a few months into the future is also of sufficient accuracy for the pipeline. However, the monitoring observations should be analyzed monthly, and the slopes of the changes over time should be updated quarterly.

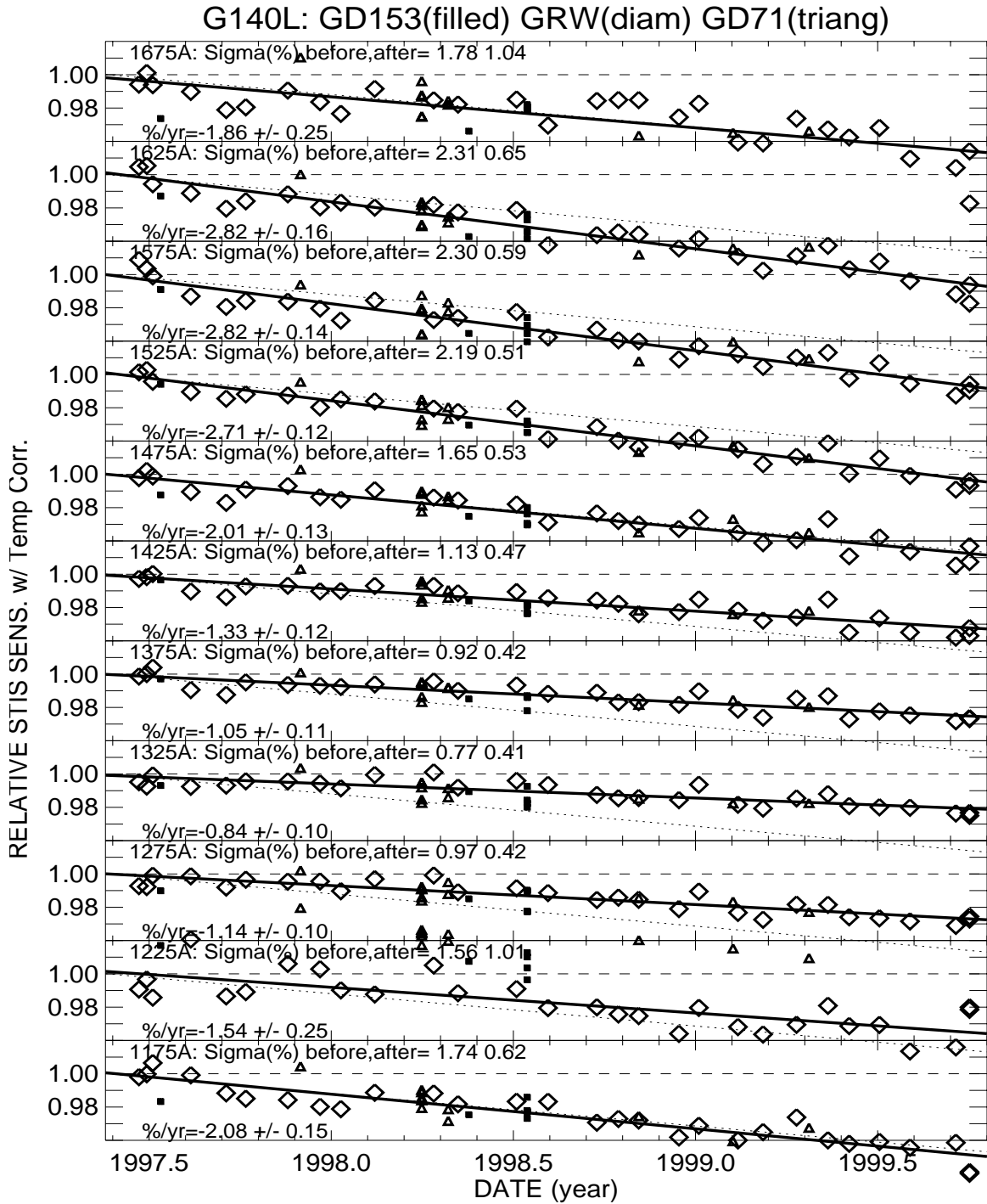
6. ACKNOWLEDGEMENT

Nolan Walborn is PI for the HST programs that obtain the monitoring observations.

7. REFERENCES

Bohlin, R., Collins, N., & Gonnella, A. 1998, Instrument Science Report, STIS 97-14, (Baltimore:STScI).

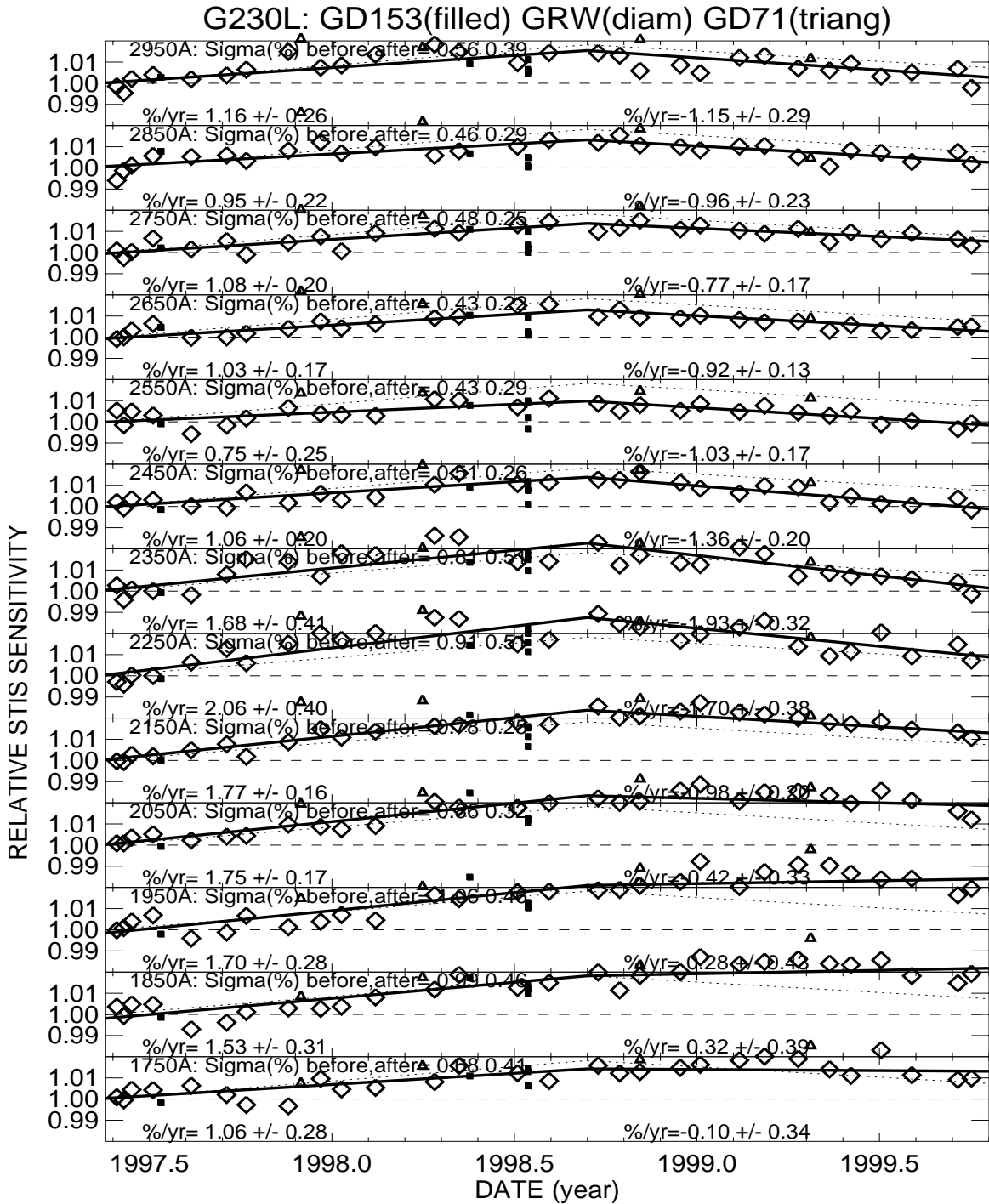
Walborn, N., & Bohlin, R. 1998, Instrument Science Report, STIS 98-27, (Baltimore:STScI).



Fit 29 DIAMONDS only

BOHLIN: MAKE-TCHANG 15-Oct-1999 16:26

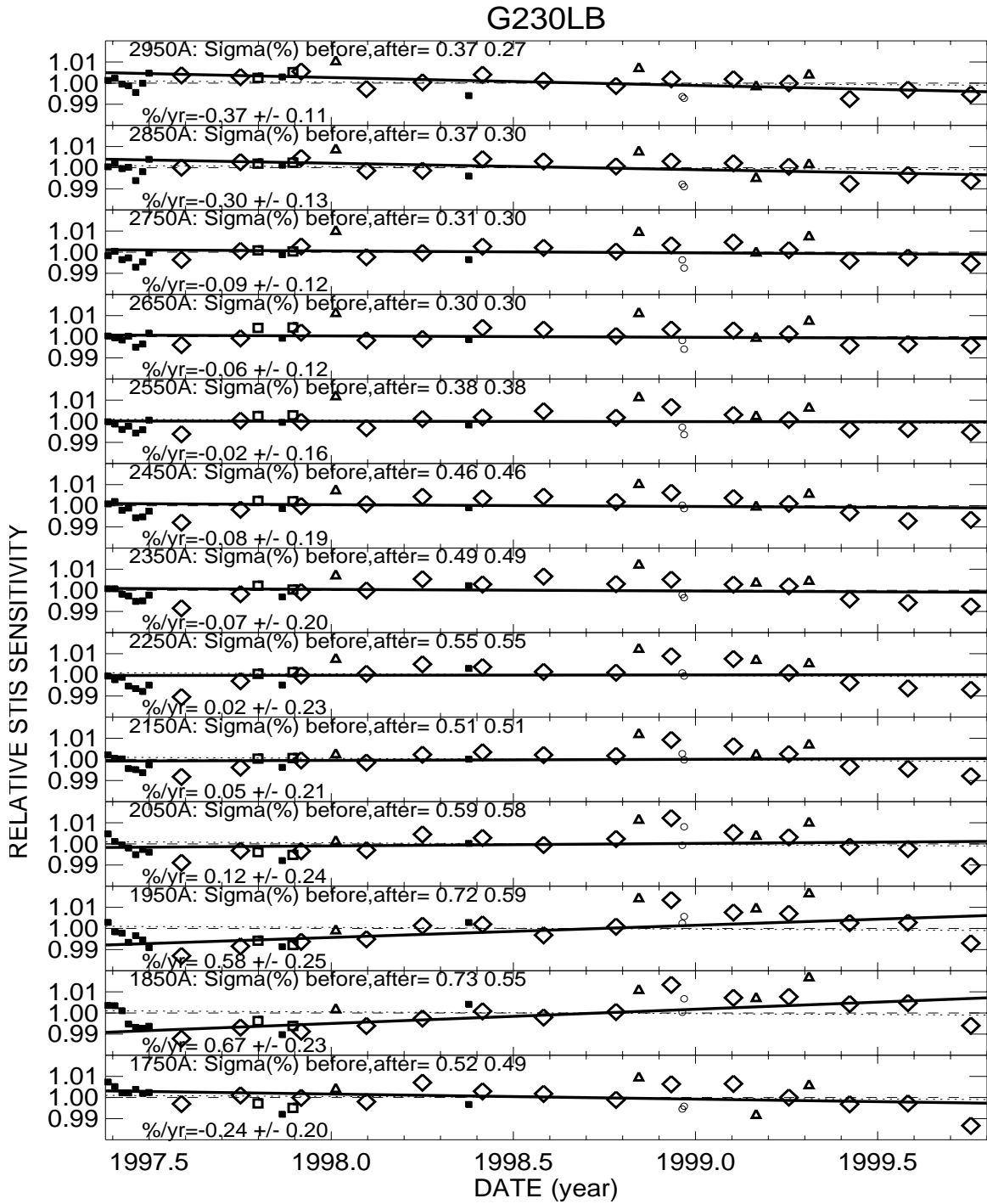
Figure 1: Relative sensitivities as a function of time and wavelength for G140L. The coefficients in %/yr for the linear fits, their 1σ uncertainty, and the 1σ rms scatter before and after correction are written on the plot. Only the large diamonds are used to define the fit and scatter. The data for the other WD stars listed at the top of the figure are for qualitative confirmation only. The light dotted lines are the fit to the average change in the broadband response of G140L.



Fit 29 DIAMONDS only

BOHLIN: MAKE-TCHANG 15-Oct-1999 16:27

Figure 2: As in Figure 1 for G230L. Two straight line fits are required with a break at 1998.7.



Fit 14 DIAMONDS only

BOHLIN: MAKE-TCHANG 15-Oct-1999 17:42

Figure 3: As in Figure 1 for G230LB.

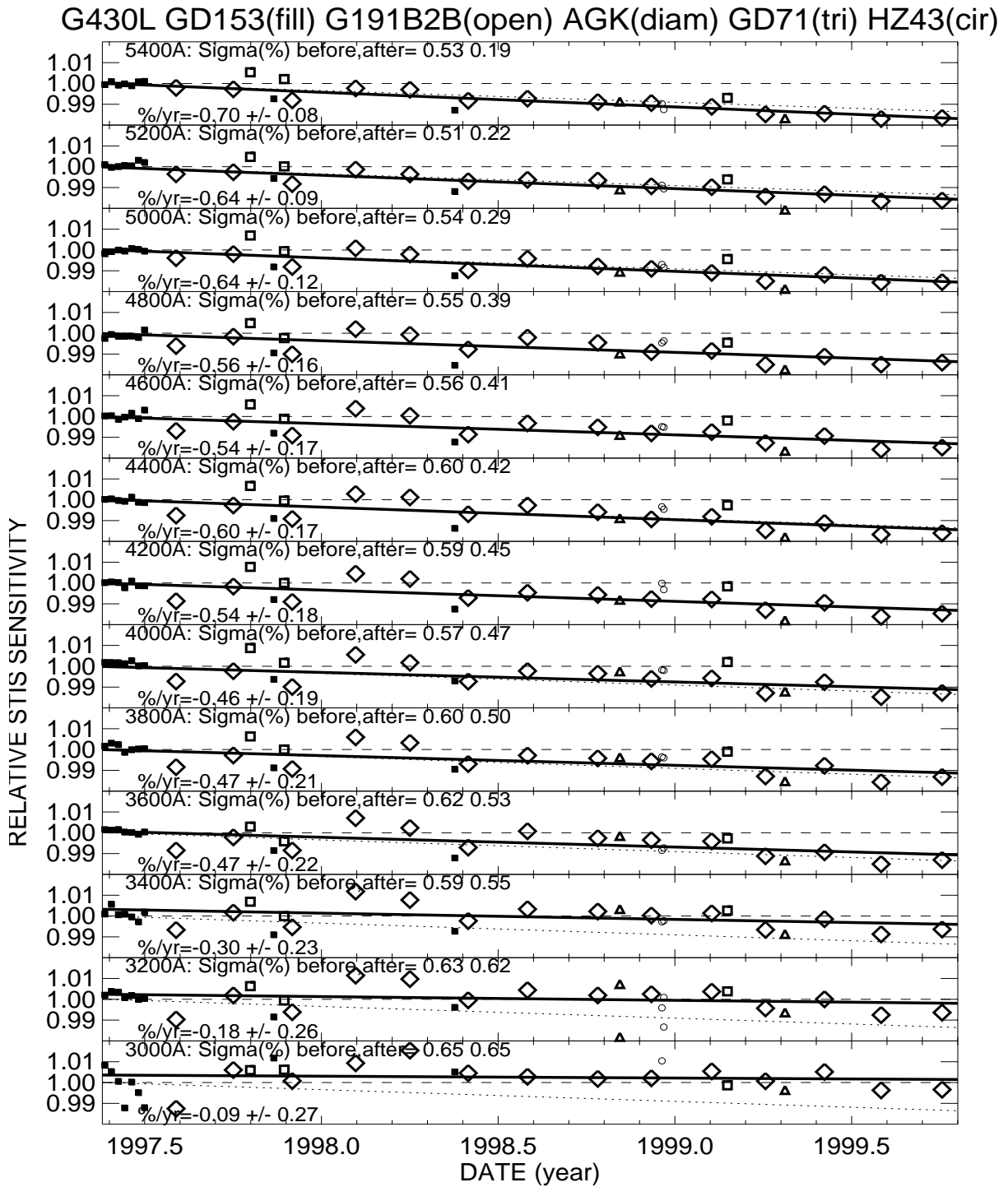
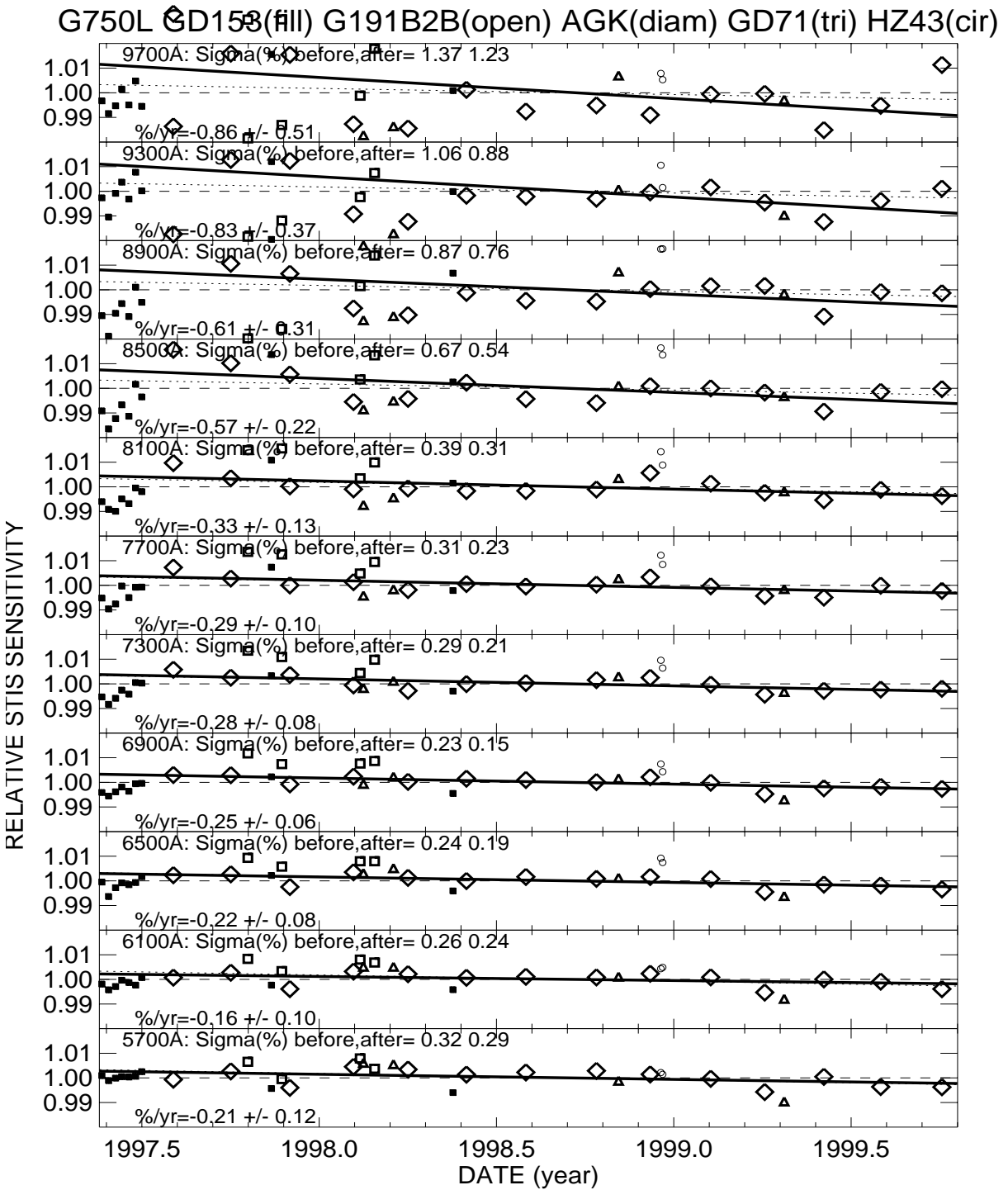


Figure 4: As in Figure 1 for G430L.



Fit 14 DIAMONDS only

BOHLIN: MAKE-TCHANG 15-Oct-1999 16:28

Figure 5: As in Figure 1 for G750L.

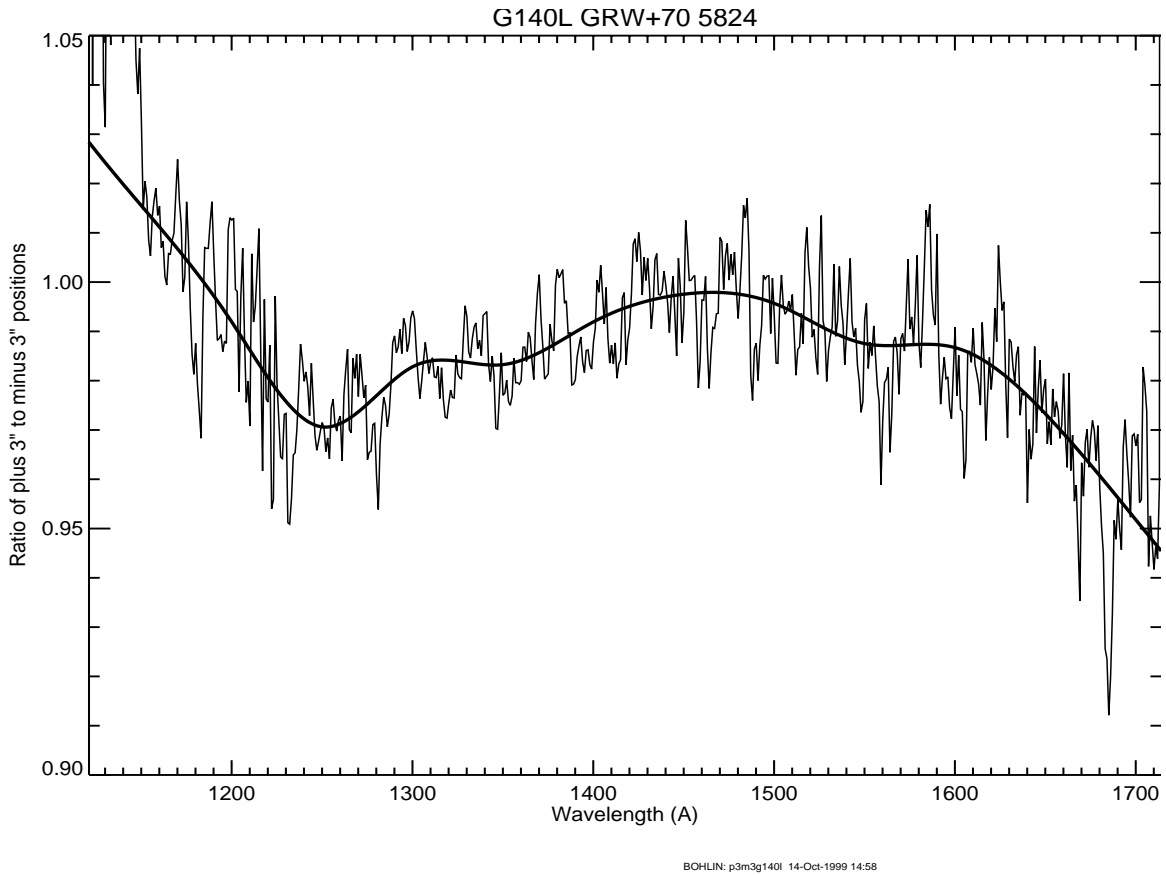


Figure 6: Ratio of the average of 22 corrected spectra of GRW+70D5824 at the position +3 arcsec above center to the average of 7 corrected spectra of GRW+70D5824 at the position -3 arcsec below center of the FUV-MAMA (noisy solid line.) A 12 node spline fit to this ratio is shown by the smooth, heavy solid line.

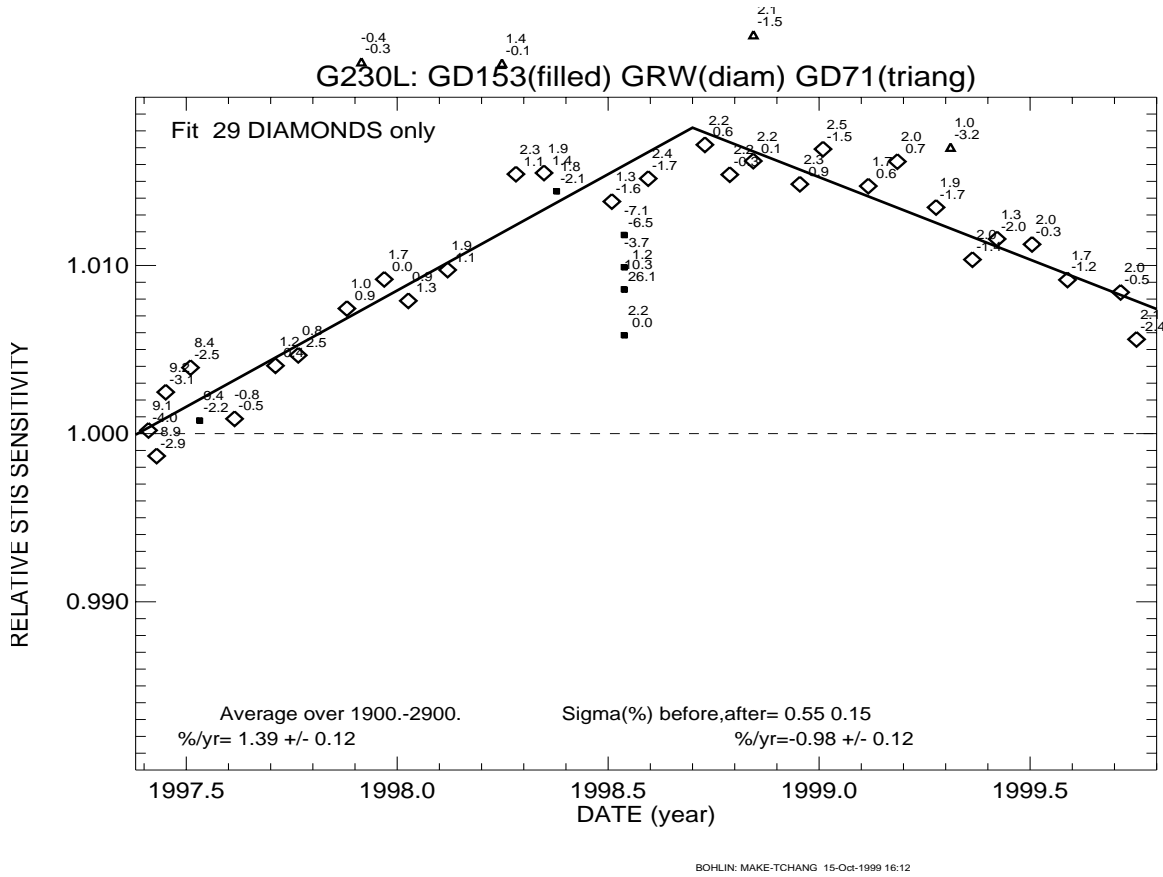


Figure 7: G230L relative sensitivity as a function of time averaged over wavelength. The pairs of numbers by each point give the x,y pixel offsets of the spectral trace with respect to the image centers, with x above and y below.

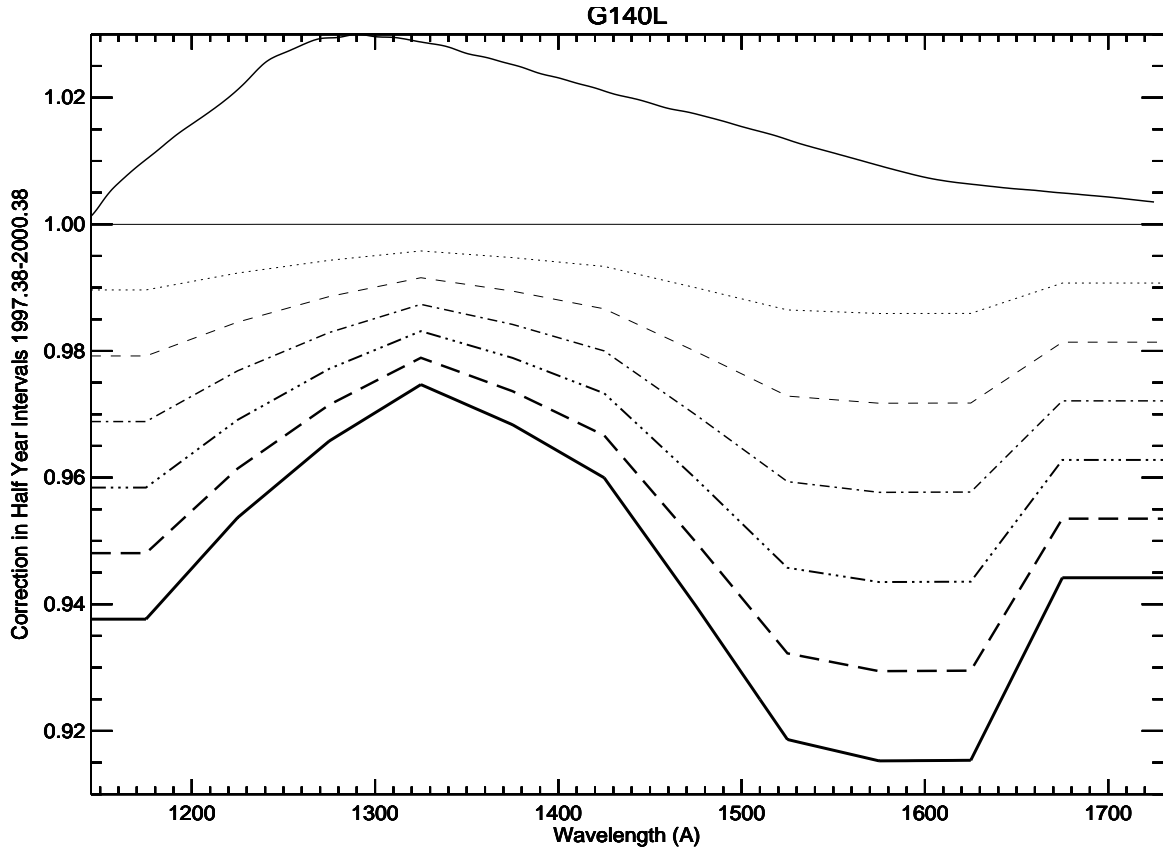


Figure 8: Wavelength dependent sensitivity change for G140L, shown every half year from 1997.38 (unit line) to 2000.38 (lowest heavy solid line.) The results for the bins at 1175 and 1675 Å are extended to the limits of wavelength coverage by the flat line segments at the wavelength extremes. The top panel (above 1.00) shows the G140L sensitivity shape, which correlates with the sensitivity change except for the last wavelength bin at 1675 Å.

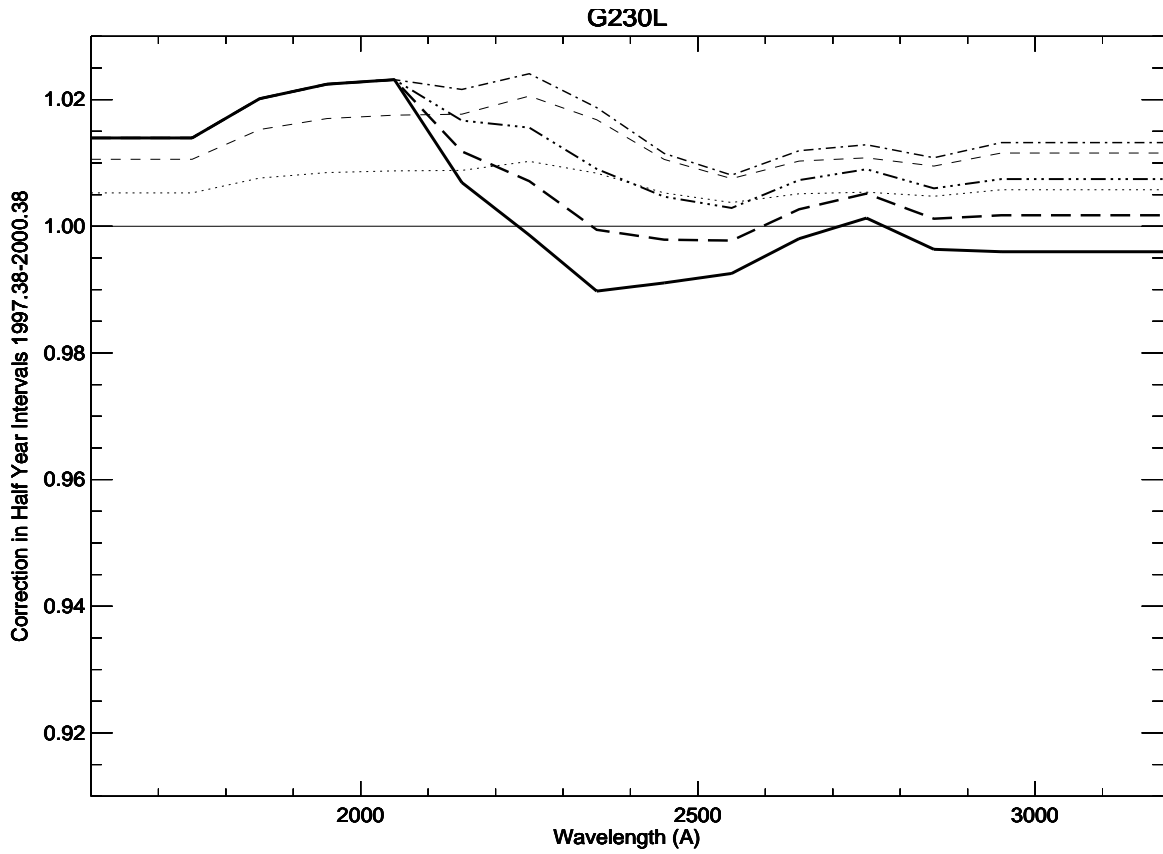


Figure 9: Wavelength dependent sensitivity change for G230L, with the same line style and boldness as in Figure 8. Only by 2000.38 is the predicted sensitivity lower than at 1997.38 at most of the longer wavelengths.

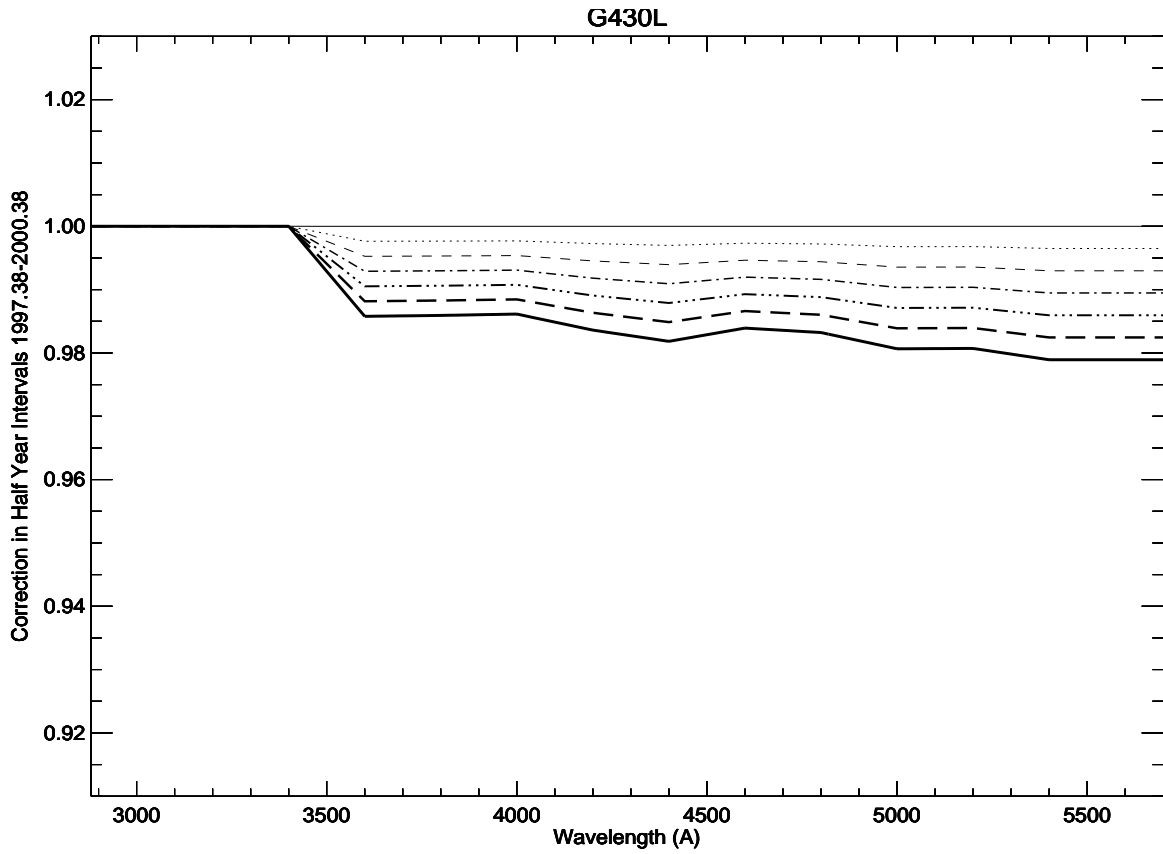


Figure 10: Wavelength dependent sensitivity change for G430L, as in Figure 8. The losses are continuous and monotonically increasing toward longer wavelengths. Only by 2000.38 does the predicted decline in response exceed 2% anywhere.